DISCRETE AND CONTINUOUS
DYNAMICAL SYSTEMS SERIES S
Volume **4**, Number **5**, October **2011**

doi:10.3934/dcdss.2011.4.1247

pp. **1247–1266**

BREATHER-MEDIATED ENERGY TRANSFER IN PROTEINS

Francesco Piazza

Laboratoire de Biophysique Statistique, EPFL-ITP-SB
BSP-720, CH-1015 Lausanne, Switzerland
Present address: Centre de Biophysique Moleculaire (CBM-CNRS)
University of Orleans
Rue Charles Sadron, 45071 Orleans, France

Yves-Henri Sanejouand

Laboratoire Biotechnologie, Biocatalyse et Biorégulation
UMR 6204 du CNRS, Faculté des Sciences et des Techniques
2, rue de la Houssinière, 44322 Nantes Cedex 3, France

Abstract. In this paper we investigate how energy is redistributed across protein structures, following localized kicks, within the framework of a nonlinear network model. We show that energy is directed most of the times to a few specific sites, systematically within the stiffest regions. This effect is sharpened as the energy of the kicks is increased, with fractions of transferred energy as high as 70 % already for kicks above 20 kcal/mol. Remarkably, we show that such site-selective, high-yield transfers mark the spontaneous formation of spatially localized, time-periodic vibrations at the target sites, acting as efficient energy-collecting centers. A comparison of our simulations with a previously developed theory reveals that such energy-pinning modes are discrete breathers, able to carry energy across the structure in an quasi-coherent fashion by jumping from site to site.

1. **Introduction.** While the chemical events and static structural features of important biological mechanisms, such as allosteric communication, have been extensively studied, little is known about how the dynamics of individual proteins shapes and regulates such phenomena [11, 45, 46]. From Dynamic NMR methods a picture seems to arise in which flexibility on microsecond to millisecond timescales is intrinsic and likely to be an essential feature of most proteins [14].

Quantitative analysis of dynamics at multiple sites of enzymes reveal large-scale collective motions, thus suggesting that large-scale vibrations such as low-frequency normal modes may embody the functional spatial correlation patterns [43]. On the other hand, the exchange of energy among collective modes in nonlinear models of proteins has been investigated, unveiling that coupling between modes strongly depend on their geometrical overlap [27]. However, little is understood about how these functionally relevant, collective movements are connected with local atomic fluctuations, which are much faster. NMR measurements have clearly shown that a full hierarchy of time scales spanning several orders of magnitude is at the basis of protein functioning. In particular, pico- to nano-second timescale fluctuations in

2000 *Mathematics Subject Classification.* Primary: 70-XX, 37-XX, 92-XX; Secondary: 70K75, 34C15, 37N25, 92C40.

Key words and phrases. Nonlinear dynamical systems, Proteins, Enzymes, Network models, Discrete Breathers, Energy transfer.

hinge, stiff regions have been shown to facilitate the large-scale, slower motions that produce functionally competent states on physiologically relevant time scales [19]. All in all, a coherent picture arises reaffirming the important connection between protein topology (i.e. their peculiar, hierarchical spatial arrangement of atoms) and dynamics, highlighting the functional role of peculiar fold-rooted vibrational patterns at different time scales [43, 35, 5].

Nonlinear effects are known since a long time to be highly relevant in protein dynamics [26, 18]. In particular, these features are now widely recognized to play an important role in energy storage and transfer processes as a consequence of ligand binding, chemical reaction, *etc* [38, 52]. As a matter of fact, completely harmonic descriptions of the allosteric motions are now accepted to be inadequate to capture the slow millisecond conformational changes, reaffirming the crucial role of hinge motions occurring in the stiffest regions in mediating between faster atomic fluctuations and slower functional rearrangements [47]. In this sense, persistent concentration of energy at specific sites would play a pivotal role in directing conformational changes at a higher level.

Among nonlinear effects, several studies have appeared maintaining that localized vibrational modes of nonlinear origin may play a leading role in providing the means for efficient energy storage in many biological processes [29]. A variety of experimental studies confirm indeed the presence of long-lived modes in proteins [52, 48, 50, 49]. For example, localized vibrations in $\alpha-$helices have been recently proposed to constitute an energy concentration channel during enzymatic catalysis [8, 12]. Along the same lines, energy transfer could also be mediated by nonlinear excitations hopping along the chain as a result of nonlinear coupling of spatially overlapping resonant localized modes [23, 24].

Different kinds of nonlinear excitations have been hypothesized to influence protein functional dynamics. These include topological excitations, such as solitons [13, 41] as well as discrete breathers (DB) [2, 22]. The latter, also known as Intrinsic Localized Modes (ILM), are time-periodic orbits found generically in nonlinear many body Hamiltonian systems [16, 40]. Their existence and stability properties are well understood at zero temperature in translationally invariant systems [3], and much work has also been done to understand the role of thermal fluctuations on DBs [36, 30, 15, 7]. However, little is known on how DB modes are affected by the interplay of spatial disorder and anharmonicity [10, 1, 33], *a fortiori* in the context of the dynamics of biological macro-molecules.

Recently, as a first-order improvement of the nowadays standard Elastic Network Model (ENM) framework [44, 4, 20, 5], we have introduced a nonlinear network model (NNM) with the aim of exploring the combined effects of nonlinearity and peculiar topology of protein scaffolds. Within the NNM framework, we have shown that long-lived, highly localized oscillations of nonlinear origin akin to discrete breathers, can form spontaneously within protein structures as a result of surface dissipation. Noteworthy, this happens with greater probability in the stiffest, deeply buried regions [21]. In this preliminary work, DBs were characterized at the end of series of molecular dynamics simulations, during wich the system was cooled down as a consequence of friction on amino acids belonging to the surface, that is, those interacting directly with solvent molecules. In a further study, we developed an analytical approach for obtaining DB solutions in the framework of NNMs. Remarkably, among their properties, we found that DBs can "jump" from site to site as their energy is lowered [31]. In this paper, we investigate the energy transfer

process that is mediated by such jumps, as it occurs in the course of microcanonical molecular dynamics simulations following an initially localized excitation.

The paper is organized as follows. In section 1, we recall the NNM model as well as our technique for calculating discrete breather orbits through a time-averaging approach [31]. In section 2, we describe our simulation and data analysis protocol, in particular the principal component analysis (PCA) of the energy redistribution process following single-site excitation. In section 3, we analyze our results and compare them with the theory described earlier. Finally, we summarize the main findings reported in this paper and illustrate the perspectives of our ongoing research.

2. **The nonlinear network model.** In the nonlinear network model (NNM), a given protein is modeled as an ensemble of N pair-wise interacting fictitious particles, each representing an amino-acid. All particles are assigned the same mass, equal to the average amino-acid mass ($M = 110$ a.m.u.) and the equilibrium coordinates $\boldsymbol{R}_i \quad (i = 1, 2, \ldots, N)$ of the corresponding α-carbon as specified in the experimentally resolved structure. Interacting pairs are identified once for all by the condition $|\boldsymbol{R}_i - \boldsymbol{R}_j| \leq R_c$, which translates into the *contact matrix* c of the network:

$$c_{ij} = \begin{cases} \theta(R_c - R_{ij}) & i \neq j \\ 0 & i = j \end{cases} \tag{1}$$

$\theta(x)$ being the Heaviside step function. Let $\boldsymbol{u}_i = \boldsymbol{r}_i - \boldsymbol{R}_i$ denote the displacement vector of the i-th residue, $\boldsymbol{r}_i$ being its instantaneous position. The NNM system potential energy reads

$$U(\boldsymbol{u}_i, \boldsymbol{u}_j) = \sum_{i>j} c_{ij} \left[\frac{k_2}{2} \left(|\boldsymbol{u}_{ij} + \boldsymbol{R}_{ij}| - R_{ij} \right)^2 + \frac{k_4}{4} \left(|\boldsymbol{u}_{ij} + \boldsymbol{R}_{ij}| - R_{ij} \right)^4 \right] \tag{2}$$

where $\boldsymbol{u}_{ij} = \boldsymbol{u}_i - \boldsymbol{u}_j$ and $R_{ij} = |\boldsymbol{R}_{ij}| = |\boldsymbol{R}_i - \boldsymbol{R}_j|$ are the inter-particle equilibrium distances. In line with our previous studies [21, 31], we fix $R_c = 10$ Å, $k_2 = 5$ kcal/mol/Å^2 and $k_4 = 5$ kcal/mol/Å^4. k_2 is chosen so that the lowest linear frequencies are in the range of what is found for actual proteins, when standard empirical energy functions are considered [28, 6, 25, 5]. Note that the choice $k_4 = 0$ in Eq. (2) amounts to building a network of Hookean central springs, that is an elastic network model [44, 4, 20, 5]. We have introduced the NNM as the simplest scheme for capturing the combined effects of spatial disorder and nonlinearity. In particular, the NNM framework is restricted to a symmetric nonlinearity. This choice allows to get rid of distinct nonlinear features associated with asymmetric terms of the potential, such as kinks and more complicated DC components of the localized modes [16], that are likely to interact with topological disorder in peculiar ways and, as such, deserve special attention in their own right.

The equations of motion for the m-th residue read

$$\ddot{\boldsymbol{u}}_m = \omega_0^2 \sum_{j>m} c_{mj} \left[1 + \frac{\ell^{-2} \left(|\boldsymbol{u}_{jm} + \boldsymbol{R}_{jm}| - R_{jm} \right)^3 - R_{jm}}{|\boldsymbol{u}_{jm} + \boldsymbol{R}_{jm}|} \right] (\boldsymbol{u}_{jm} + \boldsymbol{R}_{jm}) \tag{3}$$

where we have introduced the natural frequency $\omega_0 = \sqrt{k_2/M}$ and the length $\ell = \sqrt{k_2/k_4} = 1$ Å.

2.1. **Spatial disorder of protein networks.** The dynamics of sets of masses linked by nonlinear springs, with or without on-site potentials, has been considered in numerous studies [10, 9, 17] since the pioneering work of Fermi, Pasta and Ulam [42]. However, most of them focused on ordered, highly symmetric systems, such as linear arrays of identical masses coupled by identical springs. Studying protein NNMs provides the opportunity to consider the case of tridimensional, highly heterogeneous and disordered systems. To illustrate this point, Figure 1 shows the distribution of the number of springs linked to a given amino-acid, in the case of Subtilisin, a $N = 274$ enzyme (PDB code = 1AV7). While the average number of springs per particle is 22.4, there are particles linked by as few as 8 springs (those lying at the protein surface) while one of them is linked by as much as 38 springs (this one is deeply buried in the protein core).

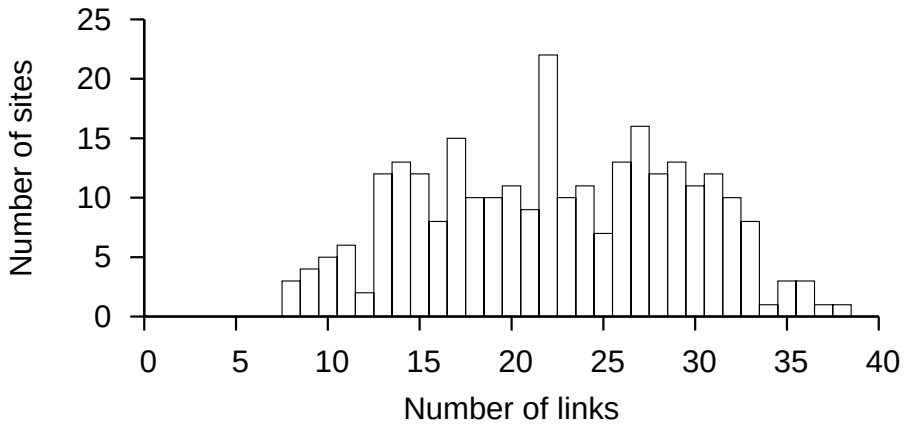

FIGURE 1. Number of sites linked by a given number of nonlinear springs, in the case of Subtilisin, an enzyme with 274 amino-acid residues. Each site is the α-carbon of a residue and two sites are linked by a nonlinear spring if they are less than $R_c = 10$ Å away from each other in the known tridimensional structure, as found in the Protein Databank (code 1AV7).

2.2. **Computing approximate breather solutions.** In ref. [31] we have introduced a technique for calculating analytically approximate breather solutions in the case of NNMs. Here, we shall examine the role of such modes in the energy transfer dynamics across a protein structure. It is then useful to recall the basics of our algorithm.

We start from a general ansatz in the form of a periodic oscillation of frequency ω, modulated by a spatially localized function of time that varies slowly on the timescale ω^{-1},

$$\boldsymbol{u}_m(t) = A\,\boldsymbol{\xi}_m(t)\cos\omega t \tag{4}$$

Further, we assume that the envelope functions $\boldsymbol{\xi}_m(t)$ are bounded and such that $\max_m \boldsymbol{\xi}_m(t) \approx \mathcal{O}(1)$, so that A sets the physical scale for the oscillation amplitude. A physically sensible DB mode centered at site k should oscillate such that $A \ll$

$\min_j R_{jk}$, that is the maximum vibration amplitude should be much smaller than the shortest bond between the k-th particle and its neighbors. The first step is then to substitute the ansatz (4) into equations (3) and expand each addendum in the sum over j to third order in A/R_{jm}. Further, we exploit the hypothesis of slowly varying envelopes, by multiplying the Taylor-expanded equations of motion by $\cos\omega t$ and performing a time average over one breather period $2\pi/\omega$. By doing so and neglecting the second time derivatives of the envelope functions, we obtain the following nonlinear algebraic system of N equations, whose $N+1$ unknowns are the time-averaged envelope patterns and the breather frequency [31]

$$\left(\frac{\omega}{\omega_0}\right)^2 \boldsymbol{\xi}_m = -\sum_{j\neq m} c_{mj}\Bigg\{\hat{\boldsymbol{R}}_{jm}(\hat{\boldsymbol{R}}_{jm}\cdot\Delta\boldsymbol{\xi}_{jm}) + \frac{3A^2}{8R_{jm}^2}\Bigg[\hat{\boldsymbol{R}}_{jm}\Big((5+2\beta R_{jm}^2)(\hat{\boldsymbol{R}}_{jm}\cdot\Delta\boldsymbol{\xi}_{jm})^3 - 3\Delta\xi_{jm}^2(\hat{\boldsymbol{R}}_{jm}\cdot\Delta\boldsymbol{\xi}_{jm})\Big) + \Delta\boldsymbol{\xi}_{jm}\Big(\Delta\xi_{jm}^2 - 3(\hat{\boldsymbol{R}}_{jm}\cdot\Delta\boldsymbol{\xi}_{jm})^2\Big)\Bigg]\Bigg\} \quad (5)$$

where we have introduced the unit distance vectors $\hat{\boldsymbol{R}}_{jm} = \boldsymbol{R}_{jm}/R_{jm}$ and the *relative* displacement patterns $\Delta\boldsymbol{\xi}_{jm} = \boldsymbol{\xi}_j - \boldsymbol{\xi}_m$. The system (5) is only apparently underdetermined, as any of the $3N$ DB components may be taken as the reference unit length. In our calculations we keep the DB amplitude $|\boldsymbol{\xi}_m| = A_B$ fixed for a guess mode centered at site m, and solve for the $3N$-set of variables $\{\boldsymbol{\xi}_1, \boldsymbol{\xi}_2, \ldots, \varphi_m, \vartheta_m, \ldots, \boldsymbol{\xi}_N, \omega_B\}$, where φ_m and ϑ_m are the azimuthal and polar angles, respectively, of the vector $\boldsymbol{\xi}_m$ and ω_B is the DB frequency. Equations (5) constitute a generalization to arbitrary topology of well known equations for approximate breather solutions in periodic lattices, which have been shown to produce accurate results in that context [39].

Equations (5) can be solved once an accurate enough guess for the DB mode is known. In ref. [31] we have shown that the Sequential Maximum Strain (SMS) algorithm provides an optimal starting point for large-amplitude breathers by computing the local maximum stiffness pattern. High-energy DBs can then be continued to low energies. However, we have also shown that it is not possible to find DB of arbitrarily low energy at every site. In fact, this is possible only at the stiffest sites, in which cases the DBs smoothly approach one of the edge spatially localized normal modes (NM). Hence, besides SMS-DBs, we shall also consider NM-DBs, that is solutions of system (5) computed by using a given edge normal mode as starting guess at low energy and then continued up to high energies. We will show in the framework of energy transfer that SMS-DBs and NM-DBs may well identify two distinct families of DBs centered at the same site.

3. **Energy transfer dynamics: Localized kicks and principal component analysis.** Thanks to the SMS algorithm, accurate guesses for highly localized DBs can be obtained for any protein site. Hereafter, we take advantage of this fact by using such localized patterns as initial conditions for standard micro-canonical molecular dynamics simulations. Each simulation starts with the following initial conditions: the protein structure being at the minimum of the potential energy surface (which, in the case of an NNM, corresponds to the PDB structure), one of its sites is "kicked", by imparting a kinetic-energy impulse of magnitude E_0

along its SMS direction. We have shown previously that when a highly localized DB is found on a protein site, the corresponding pattern of site displacements happens to be highly correlated with the pattern calculated for this site with the SMS algorithm [31]. As a consequence, kicking a site along its SMS direction has the potential to excite a DB on this site, as long as a stable DB can exist there. When it does, most of the kick energy may remain on the kicked site for long periods of time: this is one of the hallmarks of DBs. When it can not, the kick energy gets transferred to other sites.

In order to study such energy transfers, 2 ns-long simulations were performed for each kick, with a time step $dt = 0.01$ psec. The first 1 ns of simulation allows for a transient redistribution of part of the energy within the system, while the following 1 ns -long window is kept for analysis purposes. Note that for a DB with a frequency of $\omega_B = 100$ cm^{-1}, one nanosecond corresponds to nearly 3000 periods.

For characterizing correlated motions in a trajectory, a powerful tool is principal component analysis (PCA). Performed with mass-weighted site velocities, it allows to identify correlated site motions as well as their average kinetic energy. Specifically, the mass-weighted velocity covariance matrix is first built. Its elements are computed as $\langle v_k v_l \rangle$, where v_k is the velocity of coordinate k multiplied by $\sqrt{m_i}$, the mass of the corresponding site i and $\langle \cdot \rangle$ denotes a time average over the analysis timespan. This matrix is then diagonalized. Each eigenvalue yields the average kinetic energy found in a given correlated collective motion, while the corresponding eigenvector (referred to as the principal mode (PM)) provides the weight of each site coordinate for this motion.

An example of such an analysis is shown in Fig. 2, for the case of a SMS-kick of 55 kcal/mol given to residue GLU 271 of Subtilisin. Here, 13 % of the kick energy (7.2 kcal/mol) is found in a correlated motion involving mostly VAL 177, the stiffest site of Subtilisin. Note that, although this motion has catched a significant fraction of the energy fed into the system at another site, most of it has been redistributed rather evenly into the system, as expected according to the equipartition principle. However, as a further characterization of the major correlated motion found, mass-weighted velocities can be projected onto the corresponding eigenvector, the Fourier Transform of this projection giving the frequency of the motion, in this case $\omega_B = 103.3 \pm 0.5$ cm^{-1}. This value is slightly but significantly above the band-edge frequency of the linear network $\omega_E = 101.57$ cm^{-1}, a further evidence of the excitation of a DB.

Since we are interested in characterizing processes where energy self-localizes through the formation of nonlinear modes, we introduce a simple measure of localization. Let $\xi_{i\alpha}$ denote the displacement at site i in the α Cartesian direction in the mode (PM, DB or NM) $\boldsymbol{\xi}$. The localization index $\mathcal{L}_m$ of site m in the mode is defined as

$$\mathcal{L}_m = 100 \times \frac{\sum_{\alpha=x,y,z} \xi_{m\alpha}^2}{\sum_{i=1}^{N} \sum_{\alpha=x,y,z} \xi_{i\alpha}^2} \tag{6}$$

In the following, we will simply refer to the localization degree of a given mode as the localization index of its most involved particle.

Interestingly, the frequency-width of the dominant periodic component obtained through the Fourier Transform also indicates how stable is the correlated motion during the analysis timespan: the more stable the motion, the more accurate the frequency. Fig. 3 shows the frequency widths of all major correlated motions found in all SMS-kicks simulations performed in the case of Subtilisin as functions of the

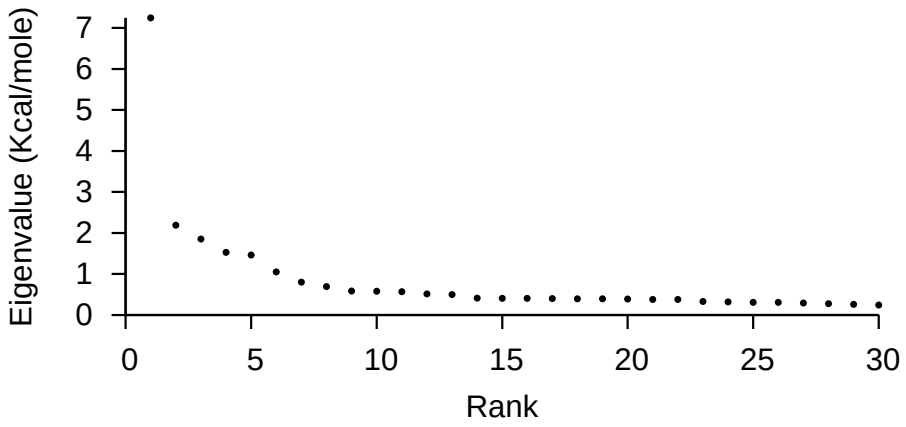

FIGURE 2. Eigenvalues of the mass-weighted velocity covariance matrix built from a 2-ns molecular dynamics simulation of Subtilisin, after a 55 kcal/mol SMS kick to the amino-acid residue 271 of Subtilisin. Only the second 1-ns window is considered for this analysis.

frequency found. Note that highest-frequency DBs, that is, those with the highest energies [21], tend to be less stable.

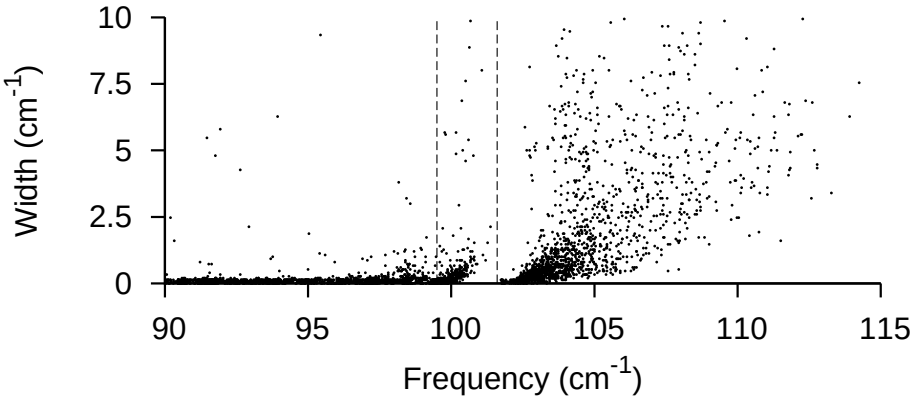

FIGURE 3. Frequency-width as a function of frequency for all dominant correlated motions found in all SMS-kicks simulations of Subtilisin for $1 \leq E_0 \leq 80$ kcal/mol. Frequency-widths are defined such that 90% of the power of the analyzed signal is included in the main periodic component. The dotted lines mark the two highest-frequency linear modes.

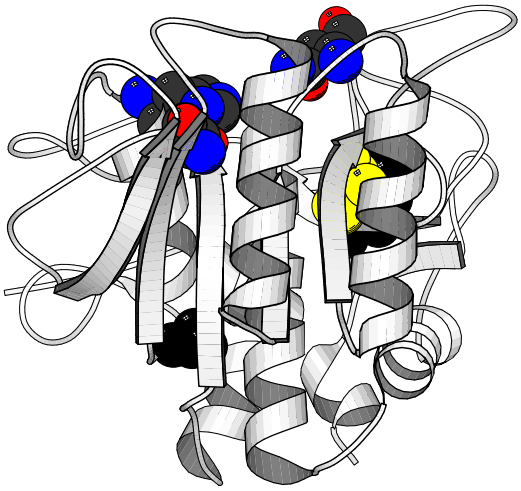

FIGURE 4. Three-dimensional structure of the enzyme Subtilisin (PDB code 1AV7). Explictly shown are a few key residues. VAL 177, the stiffest site, also the NM site of the edge normal mode (yellow), MET 199 and ALA 85 (black). Also shown in CPK color code are the catalytic residues: ASP 32, HIST 64 and ASN 155.

4. **Rationalizing energy transfer: Self-localization of non-linear modes.** In this section we examine the typical outcome of an all-site kicking dynamics in a representative case. We have probed for local relaxation of energy kicks many structures with different topologies, noteworthy including Myosin, Rhodopsin and Citrate Synthase [32]. Among all the investigated structures, we have chosen to detail herein the case of Subtilisin, a classic enzyme of the serine protease family (see Fig. 4). However, we stress that the main traits of the results described in the following are common to all enzyme structures examined so far.

When kicking all sites one-by-one, at a given energy E_0, a single location among a variable number of sites is targeted, as resolved by the most-involved site in the PM. The amount of energy transferred also depends on E_0, as determined by the corresponding ratio E_B/E_0 computed in the trajectory analysis window. Upon increasing E_0, the pool of target sites reduces in number, while the amount of the transferred energy increases, singling out a reduced number of special sites that play the role of increasingly efficient preferential target spots.

To be more quantitative, let us introduce the transfer probability to site i

$$p_i(E_0) = \frac{N_i(E_0)}{N} \tag{7}$$

where $N_i(E_0)$ is the number of transfer events to site i out of the $\sum_i N_i(E_0) = N$ kicks of energy E_0. It is instructive to compute the energy-dependent number $\mathcal{N}_{p_c}(E_0)$ of targeted sites whose cumulative transfer probability equals a given fraction p_c. While the the case $p_c = 1$ corresponds to the whole ensemble of targeted sites at each value of E_0 (in general smaller then the number of residues N), slightly

smaller values of p_c allow to gauge the degree of selectivity of energy transfer. More precisely, the threshold-dependent number of targeted sites $\mathcal{N}_{p_c}(E_0)$ is defined as the number of distinct sites that realize a fraction p_c of transfer instances at a given E_0. Indicating with $\mathcal{S}_{p_c}$ this ensemble, such definition reads

$$\sum_{i \in \mathcal{S}_{p_c}} p_i(E_0) \leq p_c \tag{8}$$

As it is clearly illustrated by Fig. 5 (a), at low energies about 80 % of the sites are targeted. As the kick energy is increased, the fraction of targeted sites decreases almost linearly to about 10 % at high energies. However, at each value of E_0, an increasingly small number of sites is targeted most of the times, while all other targeted sites correspond to increasingly rare events. This is clearly illustrated by looking at the fraction of sites that are targeted 90 % of times ($p_c = 0.9$), which drops down as a stretched exponential decay to a few units starting from about 45 % of sites that are aimed at with probability p_c.

We next turn to estimating the transfer efficiency. A fair measure can be obtained through the average fraction of transferred energy, $\langle E_B \rangle / E_0$, the averages being calculated over all N kicked residues. As it is evident from Fig. 5 (a), kicks become more and more efficient until an apparent limiting efficiency of about 35 % is attained starting from energies greater than 50 kcal/mol. Increasing E_0 further, transfer seems to become less efficient. Interestingly, such optimal transfer efficiency is attained at physiologically relevant values of the excitation energy, as for example the energy of photons absorbed by the chromophores embedded in rhodopsin within the retinal pigment [31]. However, these are average figures. Remarkably, Fig. 5 (b) shows that there exists a substantial spread in the kick efficiencies, corresponding to a steady *maximum* efficiency around 80 %.

TABLE 1. Statistics of transfer events in Subtilisin over an ensemble of 5480 single-kick simulations in the range $1 \leq E_0 \leq 80$ kcal/mol. The six higher-ranking events in the sorted list of transfer probabilities are reported for all values of the transferred energies E_B (upper half) and for $E_B > 20$ kcal/mol. Energies are expressed in kcal/mol and frequencies in cm^{-1}.

p_i (%)	Target a.a.	$\langle E_B \rangle$	$\langle \omega_B \rangle$	$\langle \mathcal{L} \rangle$ (%)	$E_B^{\max}$	$\omega_B^{\max}$	$\mathcal{L}^{\max}$
27.65	VAL 177	17.49	103.81	26.90	59.41	114.25	70.60
6.24	MET 199	8.79	100.24	23.58	43.21	104.41	71.70
5.88	ALA 85	12.10	101.13	28.59	49.23	111.91	64.68
3.96	ILE 35	6.66	96.48	14.96	48.39	108.51	64.11
3.96	ALA 153	5.20	98.95	16.37	56.92	112.28	69.79
71.12	VAL 177	29.53	105.92	38.95	59.41	114.25	70.60
9.82	ALA 85	33.60	105.77	52.06	49.23	111.91	64.68
9.36	MET 199	28.51	105.66	48.44	43.21	104.41	71.70
3.20	ILE 35	38.25	104.16	52.03	48.39	108.51	64.11
2.05	VAL 93	40.81	105.46	64.95	49.54	108.07	70.23

A few interesting figures describing the overall transfer efficiency are reported in Table 1, with reference this time to the *whole* ensemble of transfer events in the

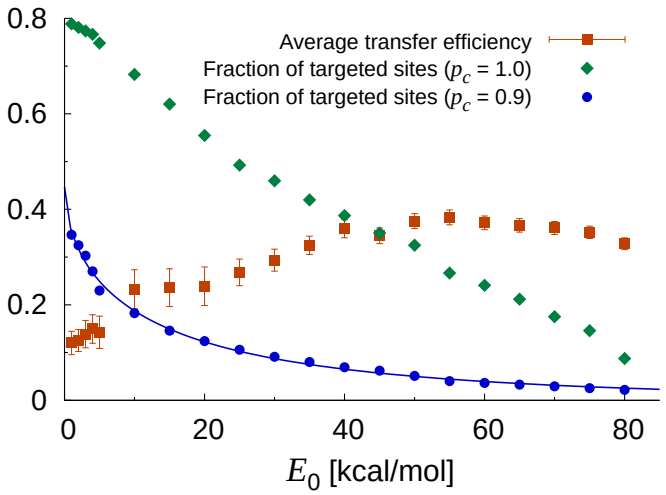

(a)

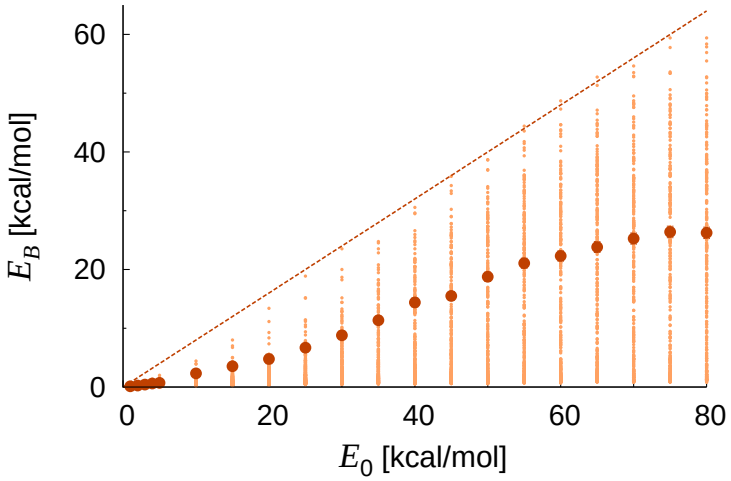

(b)

FIGURE 5. All-site analysis of energy transfer in Subtilisin. (a) Average fractions $\mathcal{N}_{p_c}(E_0)/N$ of different targeted sites at different cumulative transfer coverage p_c as calculated through formula (8) and average transfer efficiency $\langle E_B \rangle / E_0$ as functions of kick energy. The solid line is a stretched exponential fit of the form $\mathcal{N}_{0.9}(E_0) = f_0 N \exp[-(E_0/E_p)^\beta]$, with $f_0 = 0.45$, $E_p = 12.8$ kcal/mol and $\beta = 0.57$. (b) Energy found in the nonlinear localized mode as a function of kick energy for all kicked sites (small circles) along with the corresponding average values (large circles). The dashed line marks the maximum (80 %) transfer efficiency.

range $1 \leq E_0 \leq 80$ kcal/mol. Several observations are in order. It can be clearly appreciated that transfer selectivity gets sharpened at high energies. Site VAL 177 is invariably the most targeted site. However, while it appears to be excited less than 30 % of the times over the whole range of kick energies, it is singled out more than 70 % of the times by high-energy transfer events with $E_B > 20$ kcal/mol. Moreover, the average (and maximum) values of energy transferred to the less-likely targeted sites dramatically increase over the high-energy events. This means that the increased site-selectivity at high energies is also accompanied by increased local yields.

Our results show that specific energy transfer pathways exist across a protein structure and that they single out a few special target locations. Remarkably, the reduced group of sites that are excited most of the times following an SMS kick identify the stiffest regions. In fact, the ranked list of targeted residues reported in Table 1 picks out the amino acids most involved (the NM sites) in the strongly localized edge normal modes, namely, numbering from the band edge, VAL 177 (NM_1), MET 199 (NM_1,NM_5), ALA 85 (NM_3), ALA 153 (NM_4,NM_6) ILE 35 (NM_7) and VAL 93 (NM_{13}). Thus, energy transfer occurs through the spontaneous localization of vibrational energy at specific sites, following to some extent the vibrational patterns of edge NMs. The excited modes act as energy collecting centers whose efficiency strongly increases with the amount of transferred energy. This finding reinforces the picture that also emerged from spontaneous localization of energy in proteins through surface cooling. In ref. [21] we have shown that, following energy dissipation through the protein surface, a limited number of sites systematically lying in the stiffest regions end up hosting long-lived, localized vibrations of nonlinear nature. The present results reinforce the biological rationale underlying such observations: the stiffest regions is where active sites, such as catalytic sites in enzymes, are found with higher probability [21, 37]. Such interpretation is now further backed by the clear-cut observation that single-site excitations also trigger the formation of localized modes at stiff sites with high yields.

The modes that spontaneously self-localize as a consequence of a kick are characterized by well-defined frequencies, that settle well above the linear band edge as their energy increases (Fig. 6 (a)). Up to $E_B \approx 1$ kcal/mol, the excitation energy is shared by a variable number of normal modes with a poor degree of localization, signaling a rather uniform redistribution of the kick energy over the whole structure. Beyond $E_B = 10$ kcal/mol, normal modes are no longer excited following a kick, while the degree of localization of the principal mode spotlights a rapid concentration of energy at the target site (see Fig. 6 (b)). As shown in Fig. 7, the probability $P_{\omega>\omega_E}(E_0)$ of finding a frequency greater than the band edge value ω_E starts increasing beyond $E_0 \simeq 10$ kcal/mol as E_0^2, reaching an asymptotic value of about 75 %. It is important to stress that the excited modes display a single, dominant nonlinear frequency, as clearly shown by the frequency spread measured as the width of the main spectral line in the Fourier spectrum of the PM-projected system trajectories (inset of Fig. 7). As from the definition of the frequency spread, even at high energies 90 % of the total spectral power is contained within a few percent deviation from the dominant frequency.

4.1. **Discrete breathers self-excite and pin energy at the target sites.** We have seen that SMS kicks result in the spontaneous formation of strongly localized nonlinear modes at specific locations. In particular, the dispersion relation of such modes reconstructed following excitations at all sites is a remarkably well-defined

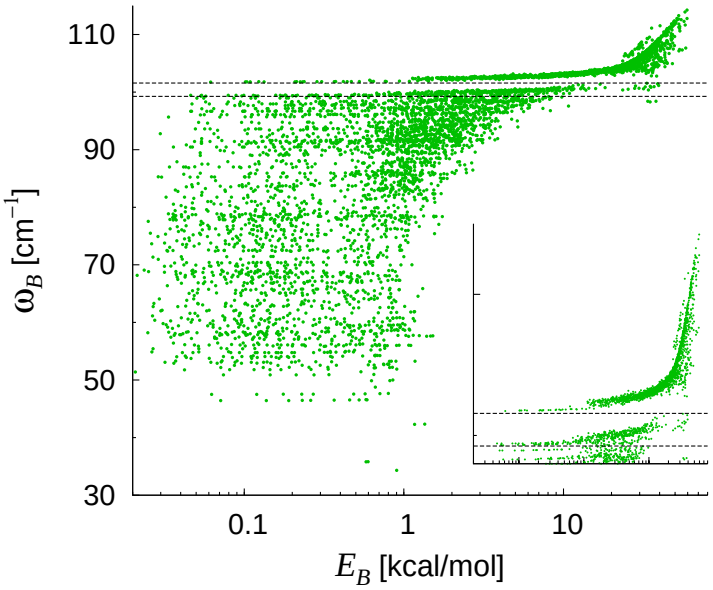

(a)

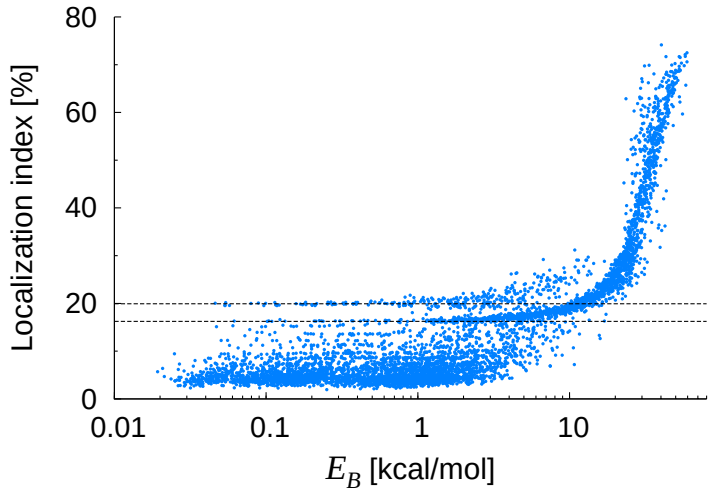

(b)

FIGURE 6. All-site analysis of energy transfer in Subtilisin. Dominant frequency (a) and localization index (b) of the excited localized modes as a function of their energy for an ensemble of 5480 kicks in the range $1 \leq E_0 \leq 80$ kcal/mol. The inset in (a) shows a close-up of the band-edge region, while the dashed lines mark the first (edge) and second higher NM frequencies. The localization indexes $\mathcal{L}_1 = 16.24$ % and $\mathcal{L}_2 = 19.93$ % of the first two edge NM modes are also marked explicitly in panel (b).

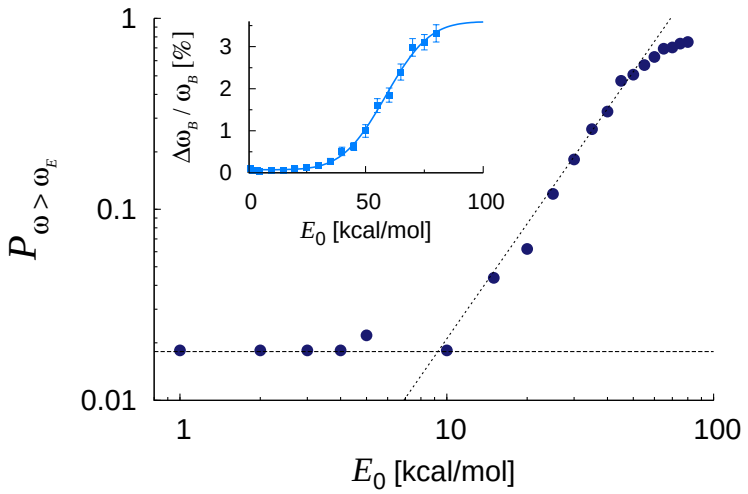

FIGURE 7. All-site analysis of energy transfer in Subtilisin. Probability of finding a frequency greater or equal to the linear band edge frequency as a function of kick energy. The horizontal line marks the energy-independent probability of exciting the edge NM (or a weak nonlinear perturbed continuation of it). The short-dashed line marks the power law $(E_0/\varepsilon)^2$, with $\varepsilon = 69$ kcal/mol. The inset shows the relative variation of the average frequency spread versus kick energy (symbols). The solid line is a guide to the eye.

one over a broad range of energies (see again Fig. 6 (a)). Furthermore, it is clear that the nonlinear modes have a tendency to *originate* from edge NMs (see inset of Fig. 6 (a)). This confirms the picture we have built in our previous study [31] of DBs in protein structures through the procedure sketched in section 2.2. One or more one-parameter families of discrete breathers exist at all sites in a given protein within the NNM framework. The majority of such DBs feature an energy gap in their excitation spectrum, whose magnitude is site-dependent, the stiffest locations harboring the DBs with smaller thresholds. Furthermore, a limited number of special DB families exist, centered at the NM sites of edge normal modes. Such breathers in general do not feature an energy gap and can be excited at arbitrarily small energies, in which regime their properties can be well described by perturbation theory of a given edge NM. While a rich palette of cases exist for DBs detaching from sub-edge modes when crossing one of the normal frequencies lying above, the DB detaching from the edge is always a gap-less mode that exists for all energies.

Our results for Subtilisin clearly show that it is the DB originating from the edge NM that is excited with increasing probability as a result of local kicks. As a matter of fact, our simulations confirm that it can be excited with finite probability even as a result of kicks of weak energy, as it can be appreciated from the low-energy portion of the probability $P_{\omega>\omega_E}(E_0)$ plotted in Fig. 7. Moreover, intra-band DBs originating from lower-lying edge modes are also excited, with frequencies lying in the gaps between consecutive linear frequencies.

The above picture can be reinforced by isolating the dispersion curves referring to energy transfers targeting a given site and comparing with the theoretical curves of DB modes centered at the same site calculated by solving Eqs. (5). Fig. 8 illustrates all transfer events to the edge NM site, VAL 177. It is clear that the entire pool of events spotlight a well-defined dispersion curve. The theoretical DB mode appears to provide an excellent description of the simulation data for E_0 greater than ≈ 20 kcal/mol, confirming that in this regime more than 70 % of the kicks end up triggering the spontaneous formation of a DB at site VAL 177 (see again Table 1). Remarkably, this means that also transfer events from faraway locations (of the order of the linear size of the protein) are possible and are equally able to trigger the spontaneous pinning of a sizable fraction of the kick energy. Discrete breathers appear thus to play the role of efficient energy-collecting centers, able to harvest the energy fed locally within distant regions.

An interesting case is offered by the transfer events that target site ALA 85, as illustrated in Fig. 9. We find that at least two families of DBs exist that are centered at this site. The DBs detaching from the third edge normal mode can be computed by solving Eqs. (5) starting from the NM pattern at low amplitudes. However, starting from the highly localized SMS guess at large amplitudes allows us to follow a different DB family. While the former kind of DBs are not sensitive to frequency crossing at ω_2 and ω_E, preserving a continuous dispersion curve and a smoothly varying vibrational pattern, the latter type of DBs are characterized by different patterns in different frequency regions (see upper panel of Fig. 9). Crossing a linear frequency causes the breather to change its pattern, while still centered at the same

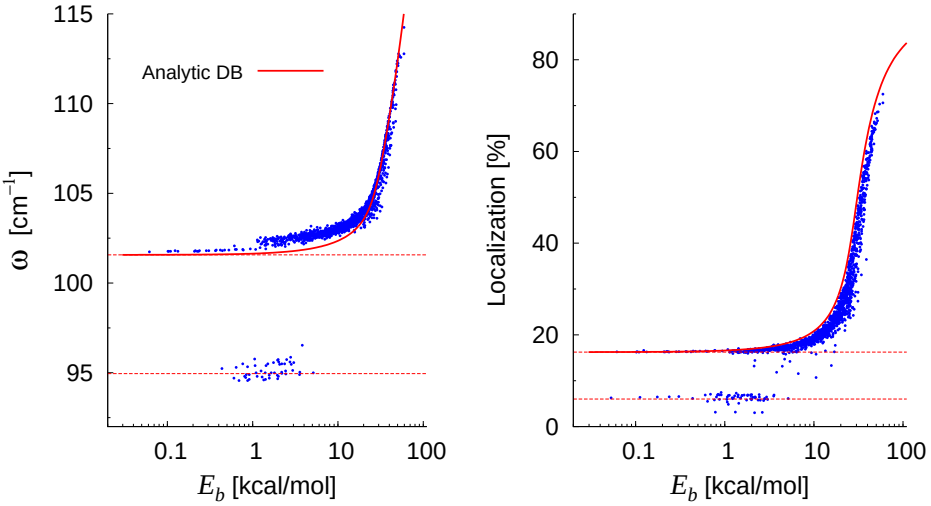

FIGURE 8. Energy transfer to VAL 177 in Subtilisin. Points mark the ensemble of all (1515) kicks resulting in the excitation of a localized mode at residue VAL 177. Solid lines represent the dispersion curve and localization plot of the approximate analytic solution centered at VAL 177. The dashed line marks the linear band edge, while dotted lines mark the frequency and localization index of the 12^{th} normal mode, which is also centered at site VAL 177.

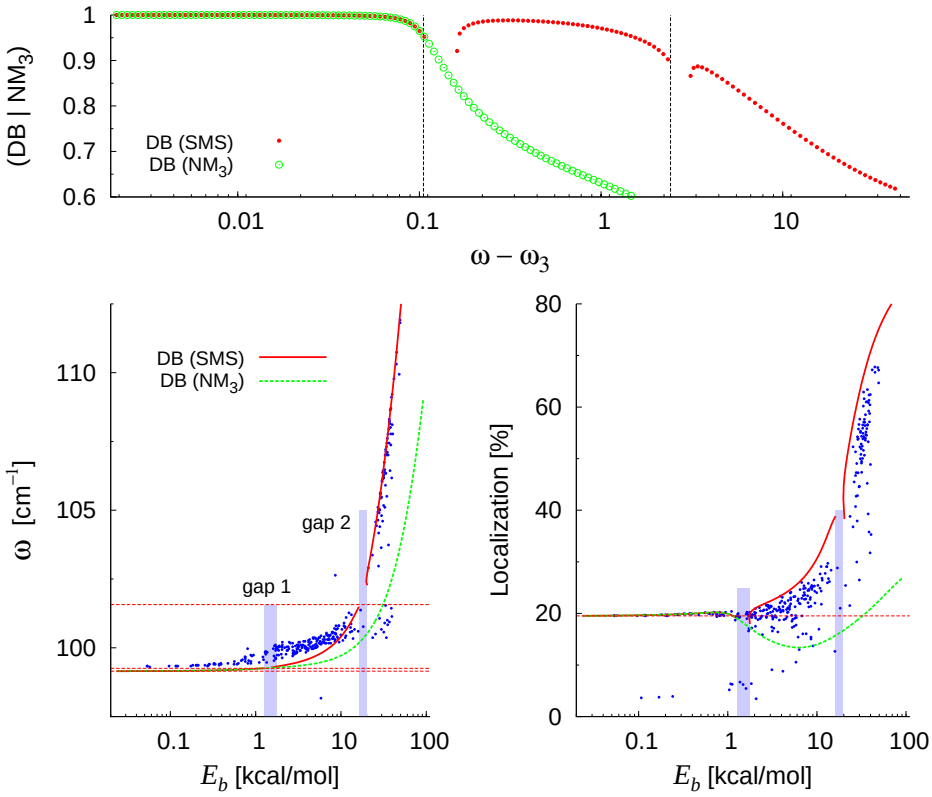

FIGURE 9. Energy transfer to ALA 85 in Subtilisin (PDB code 1AV7). Lower panels: points mark the ensemble of all (322) kicks resulting in the excitation of a localized mode at residue ALA 85. Thick lines represent the dispersion curve and localization plot of the approximate analytic solution centered at at ALA 85, computed starting from the SMS guess at large amplitudes (solid line) and starting from the 3rd edge mode at low amplitudes (dashed line). Horizontal lines mark the edge, 2nd and 3rd NM frequencies (left plot), and the localization index of the 3rd NM (right plot). The upper panel shows the normalized projection of the two DB solutions centered at ALA 85 on the 3rd NM versus frequency detuning from its frequency. Crossings of the two higher-frequency modes are indicated by vertical dashed lines.

site. As a matter of fact, crossings represent discontinuities in the DB pattern [31]. This causes the dispersion curve to feature two distinct gaps, i.e. regions where such DB do not exist. Remarkably, the kick simulations also seem to display energy regions where the self-exciting mode are not found, in agreement with our theory. In particular, its high-energy dispersion curve reveals that transfers to ALA 85 result in the excitation of modes belonging to the family that originates from the SMS guess.

5. **Conclusions and perspectives.** In this paper we have reported the outcome of an extensive study of the energy circulation dynamics in Subtilisin, a representative case of an enzyme structure. Within the framework of a nonlinear network model, we have shown that spatially localized, time-periodic modes of nonlinear origin emerge following local kick imparted at single amino acid sites. We have found that up to 80% of the kick energy can end up in the nonlinear mode, either localized at the excitation site or at a site lying elsewhere in the structure. Furthermore, the energy collected by the targeted particle can remain pinned for periods of time corresponding to several thousands of oscillation periods.

A previously developed theory of discrete breathers (DB) in nonlinear network models provides an excellent reading frame for our numerical results. In agreement with our previous results, energies of the order of 1 kcal/mol prove enough for exciting a collective motion that can be well characterized as belonging to the discrete breather family originating from the edge normal mode, invariably centered at the stiffest site in the structure [31]. At higher energies, breather excitation spectra exhibit a threshold of about 10 kcal/mol, above which the probability of observing a nonlinear mode with a frequency larger than the band edge frequency increases steadily. Such threshold is certainly protein-specific and constitutes an average value reflecting the complex heterogeneity of energy gaps displayed in general by local excitation spectra in a spatially disordered medium [31].

We have shown that the probability of finding highly energetic DBs at the stiffest sites is considerable: 71% of DBs with energies larger than 20 kcal/mol form at the stiffest site of all, VAL 177. Interestingly, the 10-20 kcal/mol energy range is a biologically relevant one, the lower bound being close to what ATP hydrolysis can provide, while amounts of energy of the order of 50 kcal/mol can be delivered to specific sites as a consequence of photon absorption by a chromophore, like in the case of rhodopsin. Taken together with the fact that stiffest sites in enzymes tend to cluster nearby their active site [51, 37, 21, 31], these findings reinforce the claim that breather-like nonlinear modes may play a significant role during enzyme catalytic reactions. In fact, the latter intrinsically involve time scales spanning several orders of magnitude and are thus likely to require some kind of energy storage at specific sites in order to regulate and direct energy circulation on the time scale of allosteric communication [19].

In fact, a *kick* in the framework of protein dynamics may be thought to arise in many ways. The aforementioned absorption of a photon in the visible, delivering an energy of several tens of kcal/mol is one example. Analogously, and ubiquitously in protein energetics, the free energy delivered when the terminal phosphate of an ATP molecule is hydrolyzed (it is an *exothermic* reaction) is about 10 kcal/mol. A possible mechanism through which such energy may be converted into mechanical work has been put forward recently [34]. The idea is that upon hydrolysis of the ATP molecule, the force due to the Coulombic repulsion of the product ions may do mechanical work on a neighboring molecular group by displacing it. Alternatively, if the ions depart from each other without exerting a direct action on nearby molecular groups, then they gain kinetic energy. This energy can, prior to dissipation into heat, be impulsively transferred in a collision with a neighboring group into mechanical work. As a matter of fact, this is a *mechanical kick* that follows ATP hydrolysis. The range of energies that can be obtained by reducing the electrostatic repulsion between the product ions (that is ADP^{-3} and HPO_4^{-2}), corresponding to a net relative displacement of 0.1 nm, is in the range of 5-7 kcal/mol [34].

So much for non-equilibrium kicks. However, the possibility that a kick arises at equilibrium has also to be taken into account. To this regard it is useful to provide a quick estimate for the average time between the occurrence of energy fluctuations exceeding a given magnitude. A back-of-the-envelope calculation is reported in the appendix, showing that the typical times over which fluctuations of the order of 10 kcal/mol are observed in localized vibrations in equilibrium conditions are in the nano- to micro-second range. These timescales are indeed compatible with protein functions, especially for what concerns allosteric communication phenomena.

We intend to continue this series of works along two main lines. At the fundamental level, we shall delve into the energy transfer process *per se*, in order to gain a clear and quantitative understanding of how energy jumps from site to site as a result of the interplay between nonlinearity and spatial heterogenity. Furthermore, we shall extend our analysis by employing more realistic models of protein dynamics, in order to explore how the properties of nonlinear modes are shaped in actual proteins within the challenging context of a cellular environment.

Appendix A. It is instructive to quantify the possibility that a kick of given magnitude arises at equilibrium. To this regard it is useful to provide a quick estimate for the average time between the occurrence of energy fluctuations exceeding a given energy. Let $\epsilon(t)$ be the time series of uncorrelated kinetic energy samples from the oscillations of an amino-acid residue in a protein. We take the sampling time to be $1/\gamma \simeq 1$ psec as a sufficiently long time lapse for recording uncorrelated samples in the case of a vibration that is localized in a small region around the amino-acid. Here γ is the friction coefficient describing the damping of the particle's oscillations. Under these hypotheses, the probability that two fluctuations greater than ϵ be separated by n sampling steps is Poissonian,

$$p(n) = \left(1 - e^{-\mathcal{C}(\epsilon)}\right) e^{-\mathcal{C}(\epsilon) n} \tag{9}$$

with

$$\mathcal{C}(\epsilon) = \int_{\epsilon}^{\infty} \mathcal{P}(\epsilon')\, d\epsilon' \tag{10}$$

The distribution of kinetic energy in three dimensions at equilibrium reads ($\beta^{-1} = k_B T$)

$$P(\epsilon) = \frac{\beta\sqrt{\beta\epsilon}}{\Gamma(3/2)}\, e^{-\beta\epsilon} \tag{11}$$

so that

$$\mathcal{C}(\epsilon) = 2\sqrt{\frac{\beta\epsilon}{\pi}}\, e^{-\beta\epsilon} + \mathrm{erfc}(\sqrt{\beta\epsilon}) \tag{12}$$

Combining equations (9) and (12), we get for the average time $\langle\tau\rangle$ between two rare fluctuations (that is such that $\beta\epsilon \gg 1 \Longrightarrow \mathcal{C}(\epsilon) \ll 1$)

$$\langle\tau\rangle = \frac{1}{\gamma}\sum_{n=0}^{\infty} n\, p(n) \simeq \frac{1}{2\gamma}\sqrt{\frac{\pi}{\beta\epsilon}}\, e^{\beta\epsilon} \tag{13}$$

Numerical estimates computed from formula (13) are reported in table 2. As it shows, the average waiting times between fluctuations in the range 5-10 kcal/mol, that is of the same order of the energy delivered by an ATP hydrolysis, are in the nano- to micro-second range.

ϵ (kcal/mol)	$\beta\epsilon$	$\langle\tau\rangle$ (sec)
5	8.5	1.4×10^{-9}
10	16.9	4.9×10^{-6}
15	25.4	1.9×10^{-2}
20	33.9	$8.0 \times 10^{+1}$

TABLE 2. Estimates of average waiting times between energy fluctuations larger than a given amplitude ϵ for a three-dimensional oscillator at equilibrium in the under-damped regime ($\gamma = 1$ psec^{-1}).

REFERENCES

[1] F. Abdullaev, O. Bang and M. P. Sorensen (eds.), "Nonlinearity and Disorder: Theory and Applications," vol. **45**, Kluwer Academic Publishers, Dordrecht, The Netherlands, 2001.

[2] J. F. R. Archilla, Yu. B. Gaididei, P. L. Christiansen and J. Cuevas, *Stationary and moving breathers in a simplified model of curved alpha–helix proteins*, Journal of Physics A: Mathematical and General, **35** (2002), 8885–8902.

[3] S. Aubry, *Discrete breathers: Localization and transfer of energy in discrete hamiltonian nonlinear systems*, Physica D: Nonlinear Phenomena, **216** (2006), 1–30.

[4] I. Bahar, A. R. Atilgan and B. Erman, *Direct evaluation of thermal fluctuations in proteins using a single-parameter harmonic potential*, Fold. Des., **2** (1997), 173–181.

[5] I. Bahar and Q. Cui (eds.), "Normal Mode Analysis: Theory and Applications to Biological and Chemical Systems," C&H/CRC Mathematical & Computational Biology Series, vol. **9**, CRC press, Boca Raton, 2005.

[6] B. R. Brooks and M. Karplus, *Harmonic dynamics of proteins: Normal modes and fluctuations in bovine pancreatic trypsin inhibitor*, Proc. Natl. Acad. Sci. USA, **80** (1983), 6571–6575.

[7] V. M. Burlakov, S. A. Kiselev and V. N. Pyrkov, *Computer-simulation of intrinsic localized modes in one-dimensional and 2-dimensional anharmonic lattices*, Physical Review B, **42** (1990), 4921–4927.

[8] F. Columbus (ed.), "Soft Condensed Matter. New Research," Nova Science Publishers, Inc., 2005.

[9] T. Dauxois, R. Khomeriki, F. Piazza and S. Ruffo, *The anti-FPU problem*, Chaos, **15** (2005), 015110.

[10] T. Dauxois, A. Litvak-Hinenzon, R. MacKay and A. Spanoudaki (eds.), "Energy Localisation and Transfer in Crystals, Biomolecules and Josephson Arrays," Advanced Series in Nonlinear Dynamics, vol. **22**, World Scientific, Singapore, 2004.

[11] A. del Sol, C. J. Tsai, B. Y. Ma and R. Nussinov, *The origin of allosteric functional modulation: Multiple pre-existing pathways*, Structure, **17** (2009), 1042–1050.

[12] F. d'Ovidio, H. G. Bohr and P.-A. Lindgård, *Solitons on H-bonds in proteins*, Journal of Physics: Condensed Matter, **15** (2003), S1699–S1707.

[13] F. d'Ovidio, H. G. Bohr and P.-A. Lindgrd, *Analytical tools for solitons and periodic waves corresponding to phonons on lennard-jones lattices in helical proteins*, Physical Review E, **71** (2005), 026606–9.

[14] J. J. Falke, *Enzymology: A moving story*, Science, **295** (2002), 1480–1481.

[15] S. Flach and G. Mutschke, *Slow relaxation and phase-space properties of a conservative system with many degrees of freedom*, Physical Review E, **49** (1994), 5018–5024.

[16] S. Flach and C. R. Willis, *Discrete breathers*, Physics Reports, **295** (1998), 181–264.

[17] S. Flach and A. V. Gorbach, *Discrete breathers – advances in theory and applications*, Physics Reports, **467** (2008), 1–116.

[18] S. Hayward, A. Kitao and N. Go, *Harmonicity and anharmonicity in protein dynamics: A normal mode analysis and principal component analysis*, Proteins, **23** (1995), 177–186.

[19] K. A. Henzler-Wildman, M. Lei, V. Thai, S. Jordan Kerns, M. Karplus and D. Kern, *A hierarchy of timescales in protein dynamics is linked to enzyme catalysis*, Nature, **450** (2007), 913–916.

[20] K. Hinsen, *Analysis of domain motions by approximate normal mode calculations*, Proteins, **33** (1998), 417–429.
[21] B. Juanico, Y.-H. Sanejouand, F. Piazza and P. De Los Rios, *Discrete breathers in nonlinear network models of proteins*, Phys. Rev. Lett., **99** (2007), 238104.
[22] G. Kopidakis, S. Aubry and G. P. Tsironis, *Targeted energy transfer through discrete breathers in nonlinear systems*, Phys. Rev. Lett., **87** (2001), 165501.
[23] D. M. Leitner, *Anharmonic decay of vibrational states in helical peptides, coils, and one-dimensional glasses*, Journal of Physical Chemistry A, **106** (2002), 10870–10876.
[24] D. M. Leitner, *Vibrational energy transfer in helices*, Phys. Rev. Lett., **87** (2001), 188102.
[25] M. Levitt, C. Sander and P. S. Stern, *Normal-mode dynamics of a protein: Bovine pancreatic trypsin inhibitor*, Int. J. Quant. Chem., **10** (1983), 181–199.
[26] R. M. Levy, D. Perahia and M. Karplus, *Molecular dynamics of an alpha-helical polypeptide: Temperature dependance and deviation from harmonic behavior*, Proc. Natl. Acad. Sci. USA, **79** (1982), 1346–1350.
[27] K. Moritsugu, O. Miyashita and A. Kidera, *Vibrational energy transfer in a protein molecule*, Physical Review Letters, **85** (2000), 3970–3973.
[28] T. Noguti and N. Go, *Collective variable description of small-amplitude conformational fluctuations in a globular protein*, Nature, **296** (1982), 776–778.
[29] M. Peyrard, "Nonlinear Excitations in Biomolecules," Springer, Berlin, 1995.
[30] M. Peyrard, *The pathway to energy localization in nonlinear lattices*, Physica D: Nonlinear Phenomena, **119** (1998), 184–199.
[31] F. Piazza and Y.-H. Sanejouand, *Discrete breathers in protein structures*, Phys. Biol, **5** (2008), 026001.
[32] F. Piazza and Y.-H. Sanejouand, *Long-range energy transfer in proteins*, Physical Biology, **6** (2009), 046014.
[33] K. O. Rasmussen, D. Cai, A. R. Bishop and N. Gronbech-Jensen, *Localization in a nonlinear disordered system*, Europhysics Letters, **47** (1999), 421–427.
[34] J. Ross, *Energy transfer from adenosine triphosphate*, The Journal of Physical Chemistry B, **110** (2006), 6987–6990.
[35] M. Rueda, P. Chacon and M. Orozco, *Thorough validation of protein normal mode analysis: A comparative study with essential dynamics*, Structure, **15** (2007), 565–575.
[36] B. Rumpf, *Growth and erosion of a discrete breather interacting with rayleigh-jeans distributed phonons*, EPL, **78** (2007), 26001.
[37] S. Sacquin-Mora, E. Laforet and R. Lavery, *Locating the active sites of enzymes using mechanical properties*, Proteins, **67** (2007), 350–359.
[38] D. E. Sagnella, J. E. Straub and D. Thirumalai, *Time scales and pathways for kinetic energy relaxation in solvated proteins: Application to carbonmonoxy myoglobin*, J. Chem. Phys., **113** (2000), 7702–7711.
[39] K. W. Sandusky, J. B. Page and K. E. Schmidt, *Stability and motion of intrinsic localized modes in nonlinear periodic lattices*, Physical Review B, **46** (1992), 6161–6168.
[40] M. Sato and A. Sievers, *Experimental and numerical exploration of intrinsic localized modes in an atomic lattice*, Journal of Biological Physics, **35** (2009), 57–72.
[41] A. Scott, *Davydov's soliton*, Physics Reports, **217** (1992), 1–67.
[42] E. Segré (ed.), "Collected Papers of Enrico Fermi," University of Chicago Press, Chicago, 1965.
[43] F. Tama and Y. H. Sanejouand, *Conformational change of proteins arising from normal mode calculations*, Protein Engineering Design and Selection, **14** (2001), 1–6.
[44] M. M. Tirion, *Large amplitude elastic motions in proteins from a single-parameter, atomic analysis*, Physical Review Letters, **77** (1996), 1905–1908.
[45] C. J. Tsai, A. del Sol and R. Nussinov, *Allostery: Absence of a change in shape does not imply that allostery is not at play*, Journal of Molecular Biology, **378** (2008), 1–11.
[46] C. J. Tsai, A. Del Sol and R. Nussinov, *Protein allostery, signal transmission and dynamics: A classification scheme of allosteric mechanisms*, Molecular Biosystems, **5** (2009), 207–216.
[47] P. C. Whitford, J. N. Onuchic and P. G. Wolynes, *Energy landscape along an enzymatic reaction trajectory: Hinges or cracks?*, HFSP Journal, **2** (2008), 61–64.
[48] S. Woutersen and P. Hamm, *Nonlinear two-dimensional vibrational spectroscopy of peptides*, Journal of Physics: Condensed Matter, **14** (2002), R1035–R1062.
[49] A. Xie, A. F. G. van der Meer and R. H. Austin, *Excited-state lifetimes of far-infrared collective modes in proteins*, Physical Review Letters, **88** (2001), 018102.

[50] A. Xie, L. van der Meer, W. Hoff and R. H. Austin, *Long-lived amide i vibrational modes in myoglobin*, Physical Review Letters, **84** (2000), 5435–5438.
[51] L. W. Yang and I. Bahar, *Coupling between catalytic site and collective dynamics: A requirement for mechanochemical activity of enzymes*, Structure, **13** (2005), 893–904.
[52] X. Yu and D. M. Leitner, *Vibrational energy transfer and heat conduction in a protein*, Journal of Physical Chemistry B, **107** (2003), 1698–1707.

Received September 2009; revised December 2009.

E-mail address: Francesco.Piazza@cnrs-orleans.fr
E-mail address: Yves-Henri.Sanejouand@univ-nantes.fr